

Article

A Simplified Approach to Modeling the Dispersion of Mercury from Precipitation to Surface Waters—The Bay of Kaštela Case Study

Igor Živković ^{1,*} , Jan Gačnik ^{1,2}, Slaven Jozić ³ , Jože Kotnik ^{1,2}, Mladen Šolić ³  and Milena Horvat ^{1,2}

¹ Department of Environmental Sciences, Jožef Stefan Institute, 1000 Ljubljana, Slovenia; jan.gacnik@ijs.si (J.G.); joze.kotnik@ijs.si (J.K.); milena.horvat@ijs.si (M.H.)

² Jožef Stefan International Postgraduate School, 1000 Ljubljana, Slovenia

³ Laboratory of Marine Microbiology, Institute of Oceanography and Fisheries, 21000 Split, Croatia; sjozic@izor.hr (S.J.); solic@izor.hr (M.Š.)

* Correspondence: igor.zivkovic@ijs.si; Tel.: +386-1-588-5465

Abstract: Wet deposition is the main source of mercury (Hg) from the atmosphere to the Earth's surface. However, the processes that govern the dispersion of deposited Hg in seawater are currently not well understood. To address this issue, total mercury (THg) concentrations in surface seawaters and precipitation were determined on a monthly basis in the Bay of Kaštela (Central Adriatic Sea). Following the assumption that deposited THg is diluted in the seawater bulk due to mixing processes, an exponential decay-like model was developed and the wet deposition of THg was normalized based on periods between precipitation events and seawater sampling. Normalized wet deposition of THg showed significant correlation with the THg gradient in surface seawater after removal of an outlier. To explain the observed outlier, further data normalization included wind data to account for enhanced seawater mixing due to strong winds. Wind-normalized THg deposition of all datapoints showed significant correlation with the THg gradient in surface seawater. The correlation showed that the THg gradient in surface seawater of $0.378 \text{ pg L}^{-1} \text{ m}^{-1}$ corresponds to THg wet deposition of 1 ng m^{-2} after including the influence of wind speed on seawater mixing.

Keywords: mercury; wet deposition; concentration gradient; seawater mixing; Adriatic Sea



Citation: Živković, I.; Gačnik, J.; Jozić, S.; Kotnik, J.; Šolić, M.; Horvat, M. A Simplified Approach to Modeling the Dispersion of Mercury from Precipitation to Surface Waters—The Bay of Kaštela Case Study. *J. Mar. Sci. Eng.* **2022**, *10*, 539. <https://doi.org/10.3390/jmse10040539>

Academic Editor: Hong Yang

Received: 10 March 2022

Accepted: 13 April 2022

Published: 14 April 2022

Publisher's Note: MDPI stays neutral with regard to jurisdictional claims in published maps and institutional affiliations.



Copyright: © 2022 by the authors. Licensee MDPI, Basel, Switzerland. This article is an open access article distributed under the terms and conditions of the Creative Commons Attribution (CC BY) license (<https://creativecommons.org/licenses/by/4.0/>).

1. Introduction

Mercury (Hg) is a toxic global contaminant, with enhanced surface ocean concentrations mainly due to anthropogenic Hg emissions [1]. Hg is emitted to the atmosphere and released into water as a result of natural sources/processes and anthropogenic activities. Hg in the atmosphere can be carried around the globe in its elemental form and later deposited onto water surface and soils [2]. From there, Hg can be re-emitted into the air or taken up into the food web. The reduction of oxidized Hg species can result in its (re)emissions to the atmosphere [1,3,4], while methylation creates the most toxic Hg species—monomethylmercury and dimethylmercury [5–7]. In general, all Hg species are considered to be chemicals of concern as they can cause adverse health effects in humans and animals through the consumption of contaminated food [8,9].

There are two pathways for Hg deposition into terrestrial and aquatic environments: dry and wet deposition. While wet deposition processes deposit mostly oxidized and particulate-bound Hg species [10], all atmospheric Hg species (oxidized, particulate-bound, and elemental) can be deposited via dry deposition [11]. Hg dry deposition is usually estimated via micrometeorological approaches, dynamic gas flux chambers, surrogate surface approaches, and litterfall/throughfall-based approaches [12]. On the contrary, Hg wet deposition is most commonly estimated by collecting and analyzing precipitation [13]. The ratio of dry vs. wet deposition is still under debate and is thought to be dependent

on local conditions and relative abundances of different atmospheric Hg species [14]. Dry deposition (especially of elemental Hg) is thought to contribute significantly to the global Hg cycle, but its magnitude is difficult to assess due to slow deposition rates and reemission [15]. Several studies on wet deposition examined its spatial or temporal distributions [16–18], the differences between urban and rural regions [16,19], meteorological influences [16,20,21], and influences of atmospheric layers (mid- and upper-atmospheric Hg scavenging) [16,21,22].

After deposition into aquatic systems, Hg is transformed into different aqueous Hg species. The depth distribution of these species has been thoroughly investigated and varies between different oceans and seas [23,24]. Nevertheless, the distribution of Hg species is mostly variable in the upper layer of the water column (<200 m depth) and near the bottom of the water column. Deep layers (>200 m depth) generally exhibit the least depth dependence of all Hg species concentrations [23].

Even though there is an abundance of Hg wet deposition studies and studies on water-column distribution of aquatic Hg species, to the best of our knowledge there are no experimental studies available that directly connect the Hg wet deposition with the Hg dispersion in the aquatic environments.

The purpose of this paper was to estimate how wet deposition of THg is dispersed in surface seawater. We wanted to test whether THg deposited on surface seawater via precipitation can be traced using measured THg concentration gradients in surface seawater. To find appropriate relation between these two parameters, we applied a simple exponential decay-like model that accounts for seawater mixing. Due to differences in precipitation collection periods and corresponding seawater sampling, we wanted to test whether THg wet deposition could be normalized by applying a common THg half-life to a surface layer or by adjusting THg half-life to account for varying wind speeds that drive seawater mixing.

2. Materials and Methods

2.1. Study Area

The Adriatic Sea is a semi-enclosed basin located in the northernmost part of the Mediterranean Sea. It is an example of an oligotrophic, phosphorus-limited sea [25]. The principal Hg sources in the Adriatic Sea include effluents from chlor-alkali plants and the discharge of the Hg-rich Isonzo/Soča River. These contributions are responsible for the observed elevated Hg concentrations in seawaters and sediments, especially in the northern part [26].

The Bay of Kaštela is a shallow bay (maximum depth 56 m) located along the eastern coast of the Central Adriatic Sea. It is connected to the adjacent Split channel through a 1.8 km-wide opening [27]. The Bay of Kaštela was contaminated by industrial and urban waste waters between 1950 and 1990. The industrial contamination source was the former chlor-alkali plant that caused elevated Hg concentrations in sediments and seawaters [26–28].

The Jadro River is the most important freshwater source in the Bay of Kaštela, carrying nutrients and contaminants from surrounding fields. Water circulation in the bay is wind-induced, with an average water-renewal time of about one month. Renewal time is usually longer during warm summer months, when freshwater inputs and wind-induced circulation are rather low. However, during strong winds, the average water renewal time can last for a duration of five days [29]. Strong continental influences can be observed in the eastern part of the bay which shows a considerably lower water exchange compared to the western part [29].

2.2. Sampling

Seawater samples were obtained at station ST101 in the Bay of Kaštela, precipitation samples for THg determinations were collected at the Institute of Oceanography and Fisheries, while the official data on the amount of precipitation and wind speed and

direction were determined at Split-Marjan station and were obtained from the Croatian Meteorological and Hydrological Service (Figure 1).

Seawater and precipitation samples for Hg analysis were collected mostly on a monthly basis between October 2014 and December 2015. Seawater was sampled from near-surface to near-bottom water layer. The sea surface microlayer was not included in the sampling, even though the top 1000 μm of the sea surface is important for the distribution of Hg and other trace metals in aqueous environments and governs exchange processes between the atmosphere and the sea [30,31]. Seawater samples were not collected in July and September 2015 (cruise not carried out), while THg in precipitation was not determined in March, April, and November 2015 (low sample volume). Two precipitation samples were collected in February 2015 to demonstrate the effect of a strong precipitation event.

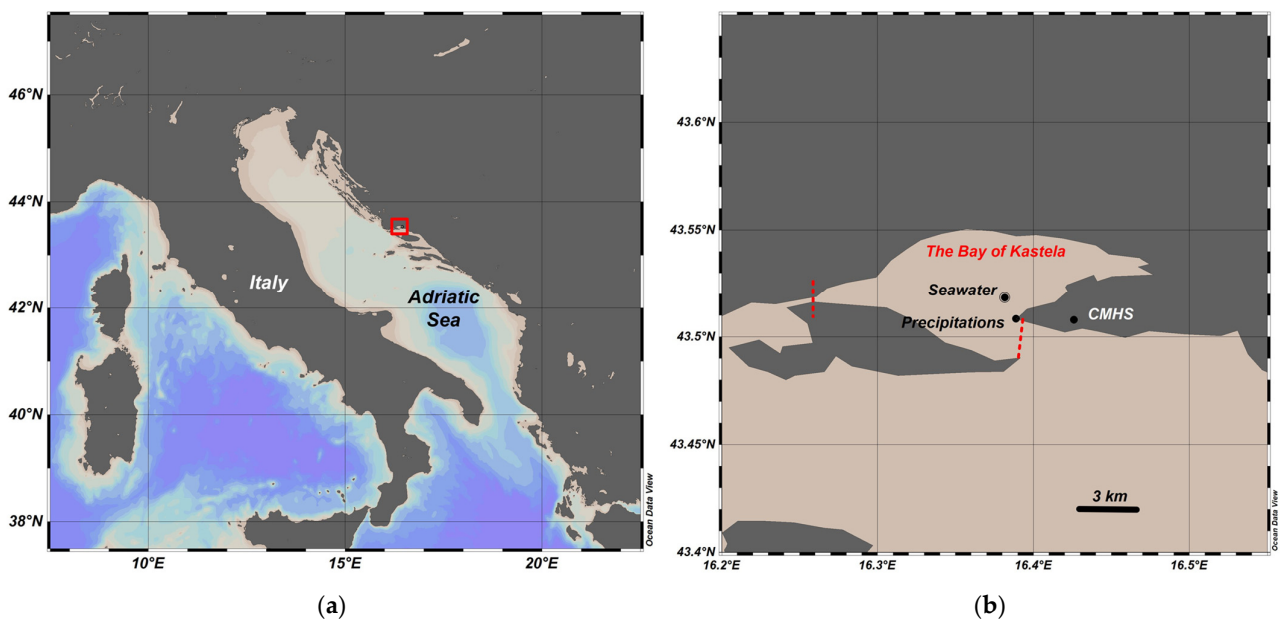


Figure 1. (a) Locations of the sampling stations in the Central Adriatic Sea marked with a red square; (b) the enlarged part of a map marked with a red square on the left panel. 'Seawater' label indicates the sampling location ST101 where seawater was sampled. 'Precipitation' label indicates the location of the Institute of Oceanography and Fisheries where precipitation samples for Hg analysis were collected. 'CMHS' label represents the location of the Croatian Meteorological and Hydrological Service station where official data on the amount of precipitation and wind speed and direction were determined. Marine borders of the Bay of Kaštela are indicated with red dotted lines. Maps were created using Ocean Data View [32].

Seawater samples were collected on board the R/V Bios Dva during monthly oceanographic cruises in the Central Adriatic Sea. Data used in this paper were extracted from a larger dataset that was previously published [33]. In short, cable-mounted Niskin bottles (5 L) were used for seawater sampling. All samples were stored in 1 L acid-cleaned borosilicate glass bottles at 5 °C until analysis. Samples for THg determinations were acidified with suprapur[®] HCl (Merck, Darmstadt, Germany) to a final content of 0.1% (*v/v*). THg in seawater samples was determined within three weeks at the Jožef Stefan Institute (Ljubljana, Slovenia) [33].

Precipitation samples for THg analysis were collected using N-CON 125 GS sampler (N-CON Systems, Arnoldsville, GA, USA) designed for the collection of wet-only mercury deposition samples. All parts of the precipitation collector that were in contact with the sample, sample bottles, and labware were cleaned prior to use. All sampling bottles (1 L) were kept in double plastic bags during transport and storage. Sampling bottles were pre-acidified with 20 mL of 2% HCl (*v/v*). The complete sample was sent to the laboratory in the sampling bottle. Samples were refrigerated at 5 °C and kept in dark.

Croatian Meteorological and Hydrological Service provided official data on the amount of precipitation and wind speed and direction, as determined at the Split-Marjan station. Precipitation data were reported as daily precipitation ($L\ m^{-2}$), while the wind data were reported as a mean hourly wind speed ($m\ s^{-1}$) and prevailing wind direction (on a 0–32 scale) at 12 m height.

2.3. THg Determination in Seawater and Precipitation

THg in seawater and precipitation was determined using cold vapor atomic fluorescence spectrometry (CVAFS; double amalgamation system; Tekran 2600, Tekran Inc., Toronto, ON, Canada) after bromine monochloride digestion, UV irradiation, pre-reduction with hydroxylammonium chloride, and reduction with tin chloride [34]. Details about the analytical performance are published elsewhere [33].

2.4. THg Gradient in Seawater

THg gradient (Γ_{0-5}) in surface seawater was defined as the difference between the THg concentrations at 0 m and 5 m depth, divided by the absolute vertical distance between these two sampling points, i.e., $\Gamma_{0-5} = (THg_{@0m} - THg_{@5m})/5\ m$. This gradient was chosen because the sedimentary input was minimal or absent at the two uppermost points of the vertical profile. Positive values of THg gradient indicate surface-water enrichment in THg as a consequence of atmospheric deposition.

2.5. Normalization of Wet Deposition

Wet deposition of THg (D_{THg} ; $ng\ m^{-2}$) is defined as the product of the amount of precipitation P ($L\ m^{-2}$) and the corresponding THg concentration ($ng\ L^{-1}$) in the precipitation. Due to the different sampling periods for each precipitation sample, we defined nominal wet deposition of THg (D_{THg}^0) as the sum of nominal daily wet deposition ($D_{THg,i}^0$). Each $D_{THg,i}^0$ was calculated as a product of the daily amount of precipitation (P_i , obtained from the Croatian Meteorological and Hydrological Service) and the average THg concentration in the precipitation sample from a given collection period (approximately one month):

$$D_{THg}^0 = \sum_i D_{THg,i}^0 = \sum_i P_i \times \overline{THg}. \tag{1}$$

As seawater sampling was performed at the end of each precipitation collection period, it is unrealistic to expect that the precipitation deposited long before seawater sampling would still be present in the surface layer at the time of seawater sampling. Therefore, it was necessary to account for seawater mixing and corresponding dilution of the deposited THg in precipitation. We defined normalized wet deposition of THg (D_{THg}^{norm}) as the sum of normalized daily wet deposition ($D_{THg,i}^{norm}$). We assumed that each $D_{THg,i}^{norm}$ follows an equivalent of the exponential decay law, i.e., that the amount of deposited THg still present at the time of seawater sampling was only a fraction of the nominal deposited THg at individual precipitation day ($D_{THg,i}^0$). The proportionality factor was in the form of exponential law, with a constant λ and the time (t_i) between the precipitation collection date and the i^{th} day prior:

$$D_{THg}^{norm} = \sum_i D_{THg,i}^{norm} = \sum_i D_{THg,i}^0 \times e^{-\lambda t} = \sum_i D_{THg,i}^0 \times 2^{-t_i / t_{1/2}}. \tag{2}$$

Exponential law is more comprehensive when considering half-life ($t_{1/2}$), i.e., the time required for THg deposition to drop to one half of the initial value of $D_{THg,i}^0$ due to seawater mixing. The value of $t_{1/2}$ was brute-forced to obtain the best agreement with the observations; the initial value was set to five days (i.e., the lowest average water renewal time for the Bay of Kaštela).

It should be noted that the model does not include basic oceanographic parameters (such as salinity and temperature) on purpose due to the model limitations to only several factors.

2.6. Wind Data and Normalization of Wet Deposition

The abovementioned normalization assumes that $t_{1/2}$ is constant during the whole precipitation collection period. However, due to the existence of an outlier obtained using this approach, we modified the $t_{1/2}$ value and assessed it based on the wind speed data. We defined wind-normalized wet deposition of THg ($D_{\text{THg}}^{\text{w-norm}}$) as the sum of wind-normalized daily wet deposition ($D_{\text{THg}, i}^{\text{w-norm}}$). We assumed that, as in the case of $D_{\text{THg}, i}^{\text{norm}}$, each $D_{\text{THg}, i}^{\text{w-norm}}$ follows an equivalent of the exponential decay law, but contains the average $t_{1/2}$ value ($\overline{t_{1/2}}$) calculated from individual $t_{1/2}$ values for each day of the precipitation collection:

$$D_{\text{THg}}^{\text{w-norm}} = \sum_i D_{\text{THg}, i}^{\text{w-norm}} = \sum_i D_{\text{THg}, i}^0 \times 2^{-t_i / \overline{t_{1/2}}} . \tag{3}$$

Drag at the surface causes wind speed reduction; wind speed at the surface exhibits a nearly logarithmic profile approximated by von Kármán–Prandtl law [35]. As the circulation in the Bay of Kaštela is wind induced, we correspondingly assumed the relation between $\overline{t_{1/2}}$ and the average daily wind speed (u_i) using an exponential function:

$$\overline{t_{1/2}} = \frac{1}{n} * \sum_i^n \eta \times e^{-\kappa \times u_i} , \tag{4}$$

where n is the number of days in the individual precipitation collection period, while η and κ are brute-forced constants used to obtain the best agreement with the observations. Using exponential function, the strongest winds would cause the shortest $t_{1/2}$ values and very rapid renewal time of the water column.

3. Results and Discussion

3.1. THg Concentrations in Precipitation

The daily amount of precipitation ranged from 0–103 L m⁻² during the course of this study (October 2014–December 2015) (Figure 2). During this period, the concentrations of THg in precipitation ranged from 2.92–38.1 ng L⁻¹ with a geometric mean of 7.74 ng L⁻¹. The largest observed value was an apparent contamination as seen from the presence of biological material (two wasps and several pine needles) in the sample. Therefore, this sample was excluded from further analysis. Excluding this sample, the concentration of THg in precipitation ranged from 2.92–16.5 ng L⁻¹ with a geometric mean of 6.70 ng L⁻¹. This range and mean are similar to those observed in precipitation from an urban and a woodland-protected area in Poland [36]. The geometric mean of THg in precipitation was also similar to the multi-year mean THg in precipitation at Iskrba station (Slovenia) and other GMOS (Global Mercury Observation System) sites in Europe [16]. The geometric mean of THg wet deposition (444 ng m⁻²) was also similar to the mean deposition of THg at European GMOS sites. The seasonal pattern followed the same pattern observed in most of the European GMOS stations; the highest THg values were determined during spring and summer seasons [16]. Contrary to these stations, the patterns of THg concentrations and the amounts of precipitation showed that the seasonal THg wet deposition maximum corresponds to the minimum in the collected amounts of precipitation (Figure 2).

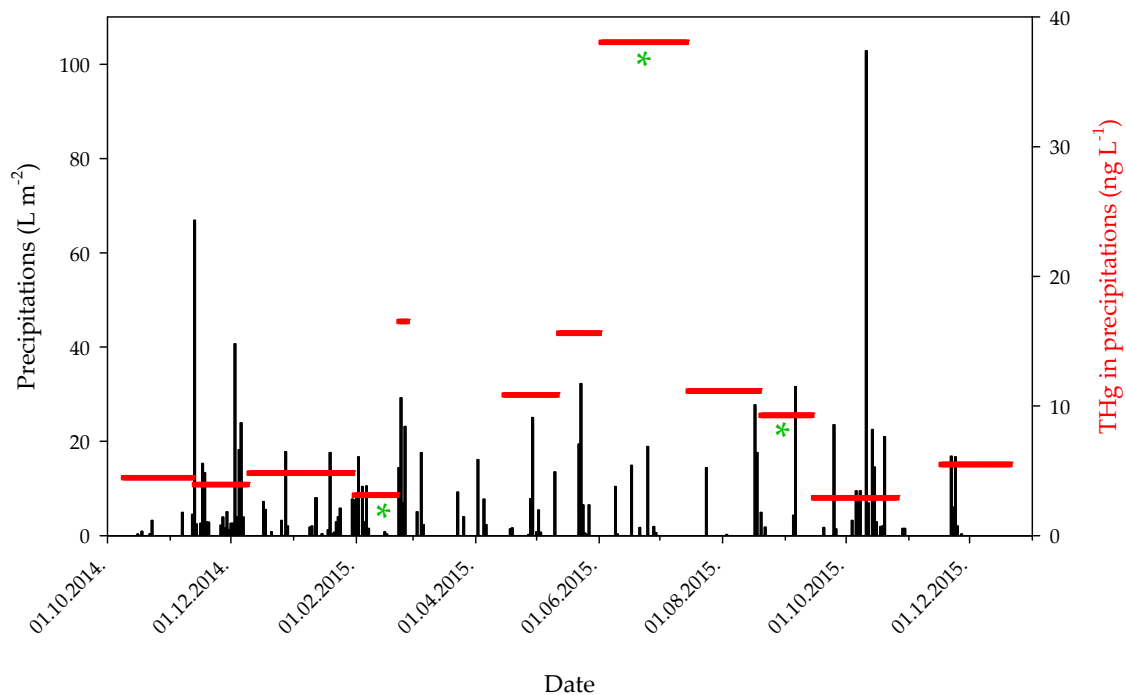


Figure 2. Daily amounts of precipitation collected at the Split-Marjan station and the average THg concentration in precipitation collected at the Institute of Oceanography and Fisheries from October 2014 to December 2015. Length of red horizontal bars indicates the precipitation collection period; the absence of the red horizontal bar indicates that THg was not determined in precipitation due to low sample volume. An asterisk indicates period without corresponding seawater sampling.

Precipitation was always in the form of rain during the study period. We assume that the increased amount of rain washed out oxidized Hg from the atmosphere, thus leaving mostly elemental Hg, which is sparingly soluble in water, present in the atmosphere. Therefore, heavy rain probably removes most of the reactive Hg from the atmosphere at the beginning, while subsequent precipitation acquires smaller Hg amounts. This decrease in THg concentration during a single rainfall event was previously demonstrated in sequential precipitation samples from Guiyang, China [37]. This might explain why the THg wet deposition minimum in the Bay of Kaštela corresponds to the maximum in the collected amount of precipitation.

3.2. THg Concentrations in Seawater

THg concentrations at station ST101 (Figure 3) were previously published as a part of a larger study [33] in which the trends and distribution of Hg fractions were discussed in detail. For the purpose of this paper, we focused only on THg concentrations in the surface layers (0 m and 5 m) and the corresponding THg gradient (Γ_{0-5}). This gradient was chosen because the sedimentary input was minimal or absent at these depths.

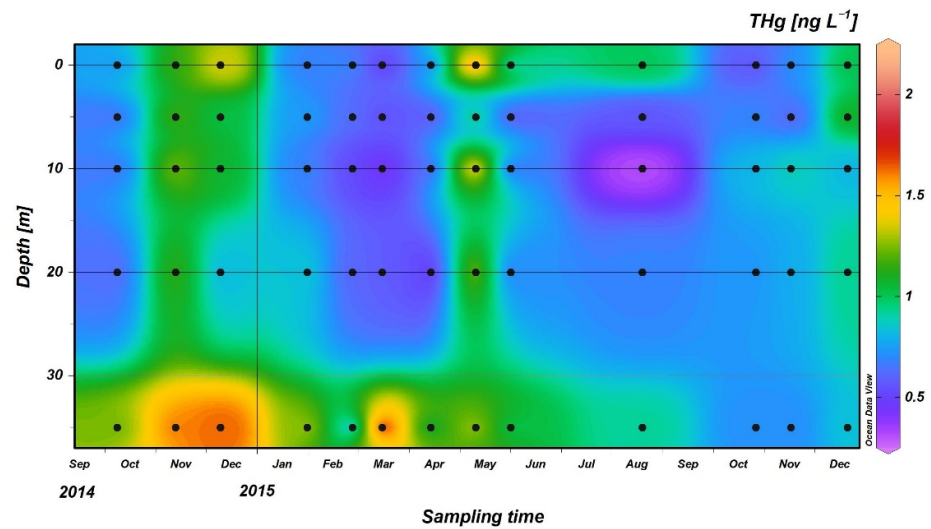


Figure 3. Vertical profiles of total mercury (THg) at station ST101 between October 2014 and December 2015. Adapted with permission from Ref. [33]. Copyright 2019, Elsevier.

The sedimentary input to the water column was limited to the lowermost water layer (35 m depth), except in November 2014 when the water column was mostly mixed. However, in most cases there was at least one more sampling depth below 5 m which had a lower THg concentration than the two uppermost sampling depths, indicating that sediment input is indeed restricted to the bottom water layer.

The effect of water mixing between precipitation and salty seawater can be observed through the vertical salinity gradients at station ST101 (Figure 4), as surface layers have lower salinity compared to underlying water layers. Additionally, the well-mixed water column in November 2014 can be easily observed through the very small vertical salinity gradient (from 36.9 to 37.4) (Figure 4).

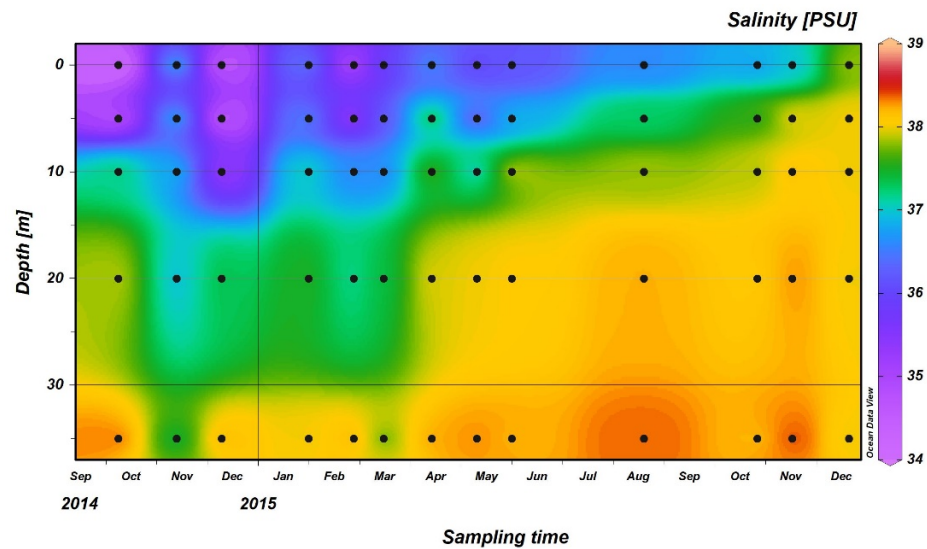


Figure 4. Vertical salinity profiles at station ST101 between October 2014 and December 2015.

Γ_{0-5} in surface seawater ranges from -30.0 to $138 \text{ pg L}^{-1} \text{ m}^{-1}$. As seen from Figure 3, the largest Γ_{0-5} value was associated with the increased THg concentration at the surface during the May 2015 sampling. The increase in surface THg concentrations was also evident during some of the other monthly samplings and probably originated from atmospheric Hg deposition. In addition, a recent study in the Adriatic Sea also showed that THg at the surface can be higher than in the closest subsurface sample [38]. Due to the presence of indi-

cations for atmospheric Hg deposition to surface seawater, we wanted to test whether this surface enrichment and THg gradient could be linked to THg concentration in precipitation.

3.3. Relations between THg in Precipitation and Seawater

There was no significant correlation between nominal THg wet deposition and THg gradient in surface seawater in the Bay of Kaštela (Figure 5a). This was expected as precipitation collection periods lasted, in general, about one month, and corresponding seawater samplings were conducted at the end of these periods. In order to relate D_{THg}^0 and Γ_{0-5} , we assumed that THg deposited prior to seawater sampling was diluted by natural mixing processes following exponential law, as described in 2.5. Using this approach, we obtained almost linear correlation between $D_{\text{THg}}^{\text{norm}}$ and Γ_{0-5} with only one outlier present (Figure 5b).

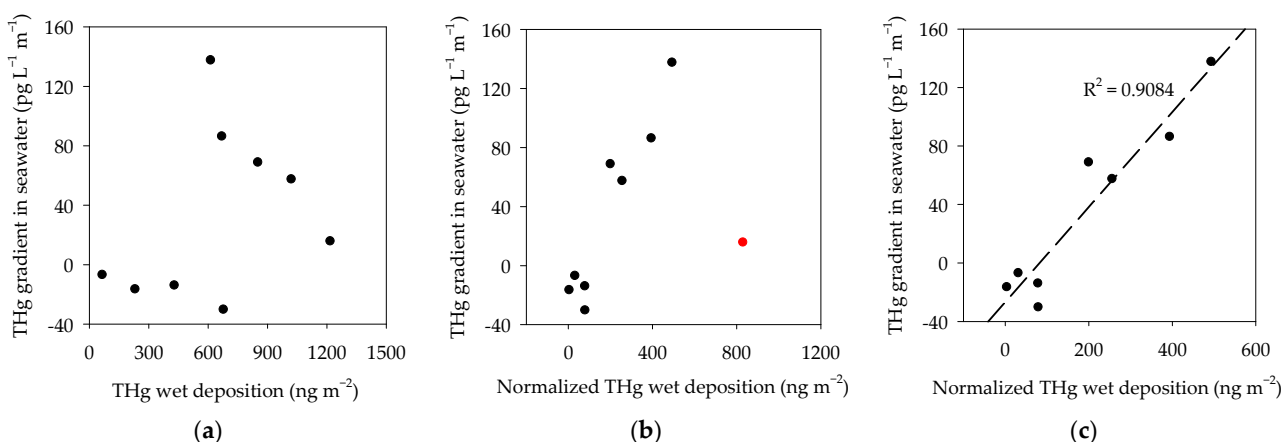


Figure 5. Correlations between THg gradient Γ_{0-5} in seawater with (a) THg wet deposition; (b) normalized THg wet deposition; and (c) normalized THg wet deposition after removal of an outlier (red point).

After the removal of this outlier, we obtained linear correlation between $D_{\text{THg}}^{\text{norm}}$ and Γ_{0-5} (Figure 5c) with R^2 value of 0.908 and slope of 0.325 m^{-2} . This result shows that there might be a simple procedure (though certainly not proven yet) for the determination of mixing half-life of deposited THg in surface waters. Based on Equation (2), we determined the $t_{1/2}$ value of 4.3 d and the corresponding λ of 0.161 d^{-1} . The $t_{1/2}$ value was slightly less than the shortest average renewal time in the whole Bay of Kaštela. This was expected, as our analysis was restricted only to surface waters at the sampling point close to the exit of the bay and considers only the time required for the removal of one half of the deposited contaminant from the surface layer.

3.4. Relation between Wind-Normalized Deposition and THg Concentration Gradient

Although there was an apparent outlier present in Figure 5b, we were aware of the reasons for such behavior. The corresponding precipitation sample was collected for only six days (Figure 2) to demonstrate the effect of a strong precipitation event. During this collection period, a relatively large amount of precipitation (73.6 L m^{-2}) containing elevated THg concentration (16.5 ng L^{-1}) was collected. However, strong winds were blowing during this period (hourly means up to 19.2 m s^{-1} ; Figure 6a) that caused severe perturbation of the water column, leading to very rapid water renewal time. The corresponding $t_{1/2}$ was therefore probably much smaller than the previously determined value of 4.3 d. To account for the effect of different wind speeds on $t_{1/2}$, we determined the $\overline{t_{1/2}}$ value (based

on individual $t_{1/2}$ values for each day of the precipitation collection) and corresponding η and κ values (Equation (4)) that fit best with the experimental data:

$$\overline{t_{1/2}} = \frac{1}{n} * \sum_i^n 10.71 \times e^{-0.421 \times u_i} \tag{5}$$

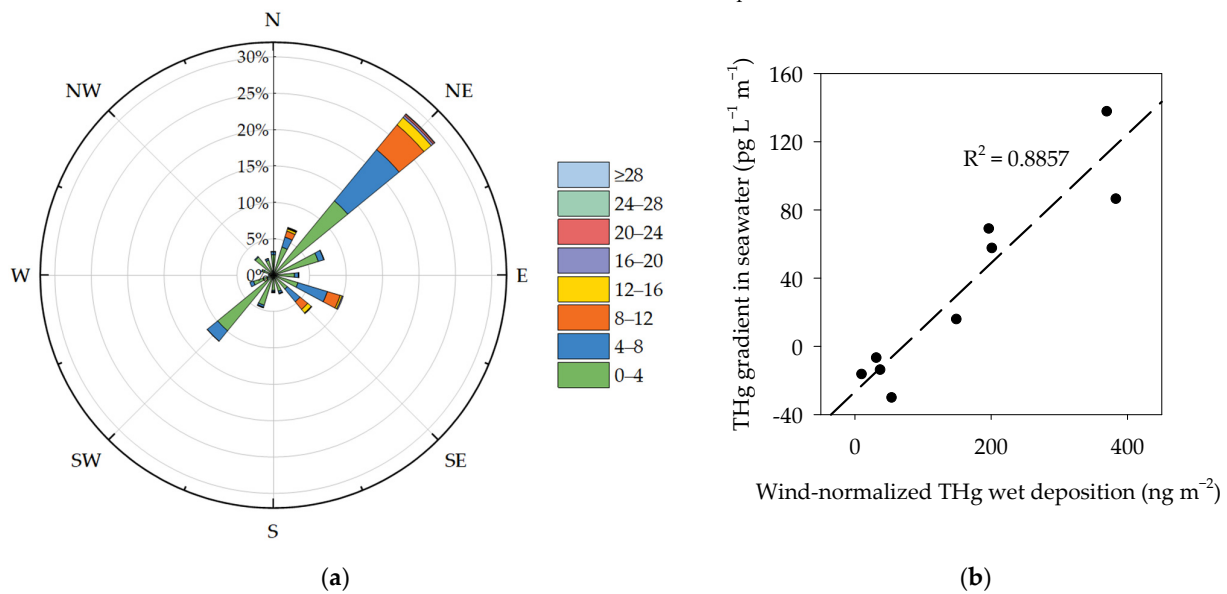


Figure 6. (a) Wind-rose diagram of mean hourly wind speeds (m s^{-1}) at the Split-Marjan station during the study period; (b) correlations between THg gradient Γ_{0-5} in seawater with wind-normalized THg wet deposition.

The $\overline{t_{1/2}}$ value was used to define wind-normalized wet deposition of THg, according to Equation (3). The obtained $D_{\text{THg}}^{\text{w-norm}}$ showed linear correlation with Γ_{0-5} for all samples (including the previously mentioned outlier) with an R^2 value of 0.886 (Figure 6b). We also tried to improve the relation between $D_{\text{THg}}^{\text{w-norm}}$ and Γ_{0-5} by incorporating wind direction into Equation (5), but the attempt was unsuccessful (data not shown). The value of the correlation line slope in Figure 6b was 0.378 m^{-2} and was slightly greater than the corresponding one obtained for correlation between $D_{\text{THg}}^{\text{norm}}$ and Γ_{0-5} . The physical representation of this value is that the THg gradient is surface seawater of $0.378 \text{ pg L}^{-1} \text{ m}^{-1}$ might be due to THg wet deposition of 1 ng m^{-2} after including the influence of wind speed on water mixing. This value might represent a characteristic of this station in the Bay of Kaštela and might describe the removal efficiency of any contaminant from the surface layer due to seawater mixing processes. However, this has to be verified by additional sampling and analysis.

3.5. Known Study Limitations

There are several limitations in this study that we were not able to address in our analysis, but we were aware of their presence. First, we were unable to include the dry deposition of THg to the surface seawater (no data). Hg dry deposition is usually estimated using models due to the lack of direct and accurate measurement methodologies [16,39]. In general, THg wet deposition rates are much bigger than the corresponding THg dry deposition rates in coastal non-urban sites, as previously determined in North America [40]. The absence of significant differences between THg deposition rates obtained using wet-only and bulk samplers in Sweden and Slovenia also corroborates this observation [41]. Therefore, we probably did not make a large error in our data analysis when determining the correlation between $D_{\text{THg}}^{\text{w-norm}}$ and Γ_{0-5} .

We also showed that sedimentary influence should be minimal at the seawater surface, but we cannot be certain of this. The other problem arises from the fact that, due to lack of

data, we did not address horizontal transport from coastal inputs. Station ST101 is close to open sea and relatively far away from neighboring cities and the Jadro River; therefore, these inputs are probably well mixed before they reach this station. One of the biggest problems arises from the fact that the daily distribution of THg in precipitation is not known, i.e., when exactly the highest amount of THg was deposited within the whole precipitation-collection period. Therefore, we could only perform data analysis using the average THg values in precipitation. A presumption that precipitation from previous months do not influence current seawater sampling was also made. This approach might be acceptable, as the longest water-renewal time in the Bay of Kaštela of about one month is similar to the average period between seawater samplings.

The influence of biota abundance, suspended particulate matter, and the deposition/sedimentation rates was also not taken into consideration (lack of data). However, future work should include these parameters as they can be important for seawater Hg exchange and transformations.

We were also not able to address THg losses from the seawater surface layer due to production of dissolved gaseous mercury, as we did not measure the concentration of elemental Hg in the air above the seawater sampling station. We performed similar analysis using data for methylated mercury (MeHg) in surface seawater and precipitation, but corresponding relations between $D_{\text{MeHg}}^{\text{w-norm}}$ with Γ_{0-5} were not obtained (data not shown), probably due to Hg methylation in seawater [42].

Diurnal variations of dissolved gaseous mercury concentrations and evasion fluxes have been previously observed in both lakes [43,44] and seawater [45]. The Hg exchange fluxes generally exhibits diurnal patterns with the largest values found around midday and the smallest values during evening/night thus following the general pattern of diurnal solar radiation variations [44,45]. The average evasion fluxes of dissolved gaseous mercury in the Adriatic Sea were previously estimated to $5.40 \text{ ng m}^{-2} \text{ h}^{-1}$ during fall [45]. However, in the current study, evasion fluxes were not considered.

Further on, the value for half-life was brute forced as there was no definite way to calculate average water renewal time in the Bay of Kaštela based on our data (data that do not include basic oceanographic parameters such as salinity and temperature). In addition, the average half-life based on wind speed was also brute forced by assuming exponential relation between individual $t_{1/2}$ for each day of the precipitation collection period and wind speed which might not be valid under all circumstances.

4. Conclusions

This study presents a simple contribution towards more accurate and detailed modeling of Hg distribution in seawater and atmosphere–water exchange. The potential of this model is promising due to its simple tracking of Hg wet deposition in the surface seawater using only THg concentrations and wind-speed data. We demonstrated that wind-normalized wet deposition of THg correlates with THg gradient in surface seawaters. The obtained regression slope might represent a characteristic of this station in the Bay of Kaštela and might describe the removal efficiency of other contaminants. The main limitation of this study is the fact that the described model and dynamic processes were overly simplified as they did not take several parameters into consideration (due to lack of data). The main limitations include lack of Hg dry deposition data and daily distribution of THg in precipitation, the unknown influences of sedimentary input, biota abundance, suspended particulate matter, deposition/sedimentation rates, evasion of produced dissolved gaseous mercury, and brute forcing of certain parameters. Nevertheless, this study provides a small contribution to future elucidation of processes that govern the atmosphere–seawater exchange of mercury.

Author Contributions: Conceptualization, I.Ž., M.Š. and M.H.; methodology, I.Ž. and S.J.; validation, I.Ž., J.G., S.J., J.K., M.Š. and M.H.; formal analysis, I.Ž. and J.G.; resources, M.Š. and M.H.; data curation, J.G., J.K., M.Š. and M.H.; writing—original draft preparation, I.Ž. and J.G.; writing—review and editing, J.K., S.J., M.Š. and M.H.; visualization, I.Ž.; supervision, M.Š. and M.H.; project

administration, M.Š. and M.H.; funding acquisition, M.Š. and M.H. All authors have read and agreed to the published version of the manuscript.

Funding: This research was funded by the Slovenian Research Agency, grant numbers P1-0143, PR-06179, J1-8156, J1-1716, J1-3033-1; European Commission, grant numbers FP7-265113—GMOS, 689443—ERA-PLANET (iGOSP).

Institutional Review Board Statement: Not applicable.

Informed Consent Statement: Not applicable.

Data Availability Statement: The data presented in this study are available in the article.

Acknowledgments: The authors would like to thank Vesna Fajon and the crew of the R/V Bios Dva for help during sample collection. We would like to thank the Physical Oceanography Laboratory at the Institute of Oceanography and Fisheries (Split, Croatia) for providing salinity data and to the Croatian Meteorological and Hydrological Service for providing precipitation and wind data.

Conflicts of Interest: The authors declare no conflict of interest. The funders had no role in the design of the study; in the collection, analyses, or interpretation of data; in the writing of the manuscript; or in the decision to publish the results.

References

- Baumann, Z.; Jonsson, S.; Mason, R.P. Geochemistry of mercury in the marine environment. In *Encyclopedia of Ocean Sciences*; Cochran, J.K., Bokuniewicz, H., Yager, P., Eds.; Elsevier: Amsterdam, The Netherlands, 2019; pp. 301–308. ISBN 9780080983004.
- UNEP. *Global Mercury Assessment 2018*; UN Environment Programme, Chemicals and Health Branch: Geneva, Switzerland, 2018.
- Zhu, S.; Zhang, Z.; Žagar, D. Mercury transport and fate models in aquatic systems: A review and synthesis. *Sci. Total Environ.* **2018**, *639*, 538–549. [[CrossRef](#)] [[PubMed](#)]
- Obrist, D.; Kirk, J.L.; Zhang, L.; Sunderland, E.M.; Jiskra, M.; Selin, N.E. A review of global environmental mercury processes in response to human and natural perturbations: Changes of emissions, climate, and land use. *Ambio* **2018**, *47*, 116–140. [[CrossRef](#)] [[PubMed](#)]
- Regnell, O.; Watras, C.J. Microbial mercury methylation in aquatic environments: A critical review of published field and laboratory studies. *Environ. Sci. Technol.* **2019**, *53*, 4–19. [[CrossRef](#)]
- Parks, J.M.; Johs, A.; Podar, M.; Bridou, R.; Hurt, R.A.; Smith, S.D.; Tomanicek, S.J.; Qian, Y.; Brown, S.D.; Brandt, C.C.; et al. The genetic basis for bacterial mercury methylation. *Science* **2013**, *339*, 1332–1335. [[CrossRef](#)] [[PubMed](#)]
- Munson, K.M.; Lamborg, C.H.; Boiteau, R.M.; Saito, M.A. Dynamic mercury methylation and demethylation in oligotrophic marine water. *Biogeosciences* **2018**, *15*, 6451–6460. [[CrossRef](#)]
- Tamele, I.J.; Vázquez Loureiro, P. Lead, mercury and cadmium in fish and shellfish from the Indian Ocean and Red Sea (African Countries): Public health challenges. *J. Mar. Sci. Eng.* **2020**, *8*, 344. [[CrossRef](#)]
- Vieira, H.C.; Rodrigues, A.C.M.; Soares, A.M.V.M.; Abreu, S.; Morgado, F. Mercury accumulation and elimination in different tissues of zebrafish (*Danio rerio*) exposed to a mercury-supplemented diet. *J. Mar. Sci. Eng.* **2021**, *9*, 882. [[CrossRef](#)]
- Lyman, S.N.; Cheng, I.; Gratz, L.E.; Weiss-Penzias, P.; Zhang, L. An updated review of atmospheric mercury. *Sci. Total Environ.* **2020**, *707*, 135575. [[CrossRef](#)]
- Enrico, M.; Le Roux, G.; Maruszczak, N.; Heimbürger, L.-E.; Claustres, A.; Fu, X.; Sun, R.; Sonke, J.E. Atmospheric mercury transfer to peat bogs dominated by gaseous elemental mercury dry deposition. *Environ. Sci. Technol.* **2016**, *50*, 2405–2412. [[CrossRef](#)]
- Wright, L.P.; Zhang, L.; Marsik, F.J. Overview of mercury dry deposition, litterfall, and throughfall studies. *Atmos. Chem. Phys.* **2016**, *16*, 13399–13416. [[CrossRef](#)]
- Sprovieri, F.; Pirrone, N.; Bencardino, M.; D’Amore, F.; Carbone, F.; Cinnirella, S.; Mannarino, V.; Landis, M.; Ebinghaus, R.; Weigelt, A.; et al. Atmospheric mercury concentrations observed at ground-based monitoring sites globally distributed in the framework of the GMOS network. *Atmos. Chem. Phys.* **2016**, *16*, 11915–11935. [[CrossRef](#)] [[PubMed](#)]
- Fu, X.W.; Zhang, H.; Yu, B.; Wang, X.; Lin, C.-J.; Feng, X.B. Observations of atmospheric mercury in China: A critical review. *Atmos. Chem. Phys.* **2015**, *15*, 9455–9476. [[CrossRef](#)]
- Gustin, M.S. Exchange of Mercury between the Atmosphere and Terrestrial Ecosystems. In *Environmental Chemistry and Toxicology of Mercury*; John Wiley & Sons, Inc.: Hoboken, NJ, USA, 2011; pp. 423–451.
- Sprovieri, F.; Pirrone, N.; Bencardino, M.; D’Amore, F.; Angot, H.; Barbante, C.; Brunke, E.G.; Arcega-Cabrera, F.; Cairns, W.; Comero, S.; et al. Five-year records of mercury wet deposition flux at GMOS sites in the Northern and Southern hemispheres. *Atmos. Chem. Phys.* **2017**, *17*, 2689–2708. [[CrossRef](#)]
- Weiss-Penzias, P.S.; Gay, D.A.; Brigham, M.E.; Parsons, M.T.; Gustin, M.S.; ter Schure, A. Trends in mercury wet deposition and mercury air concentrations across the U.S. and Canada. *Sci. Total Environ.* **2016**, *568*, 546–556. [[CrossRef](#)]
- Zhou, H.; Zhou, C.; Hopke, P.K.; Holsen, T.M. Mercury wet deposition and speciated mercury air concentrations at rural and urban sites across New York state: Temporal patterns, sources and scavenging coefficients. *Sci. Total Environ.* **2018**, *637–638*, 943–953. [[CrossRef](#)]

19. Lynam, M.M.; Dvonch, J.T.; Barres, J.A.; Landis, M.S.; Kamal, A.S. Investigating the impact of local urban sources on total atmospheric mercury wet deposition in Cleveland, Ohio, USA. *Atmos. Environ.* **2016**, *127*, 262–271. [[CrossRef](#)]
20. Holmes, C.D.; Krishnamurthy, N.P.; Caffrey, J.M.; Landing, W.M.; Edgerton, E.S.; Knapp, K.R.; Nair, U.S. Thunderstorms increase mercury wet deposition. *Environ. Sci. Technol.* **2016**, *50*, 9343–9350. [[CrossRef](#)]
21. Kaulfus, A.S.; Nair, U.; Holmes, C.D.; Landing, W.M. Mercury wet scavenging and deposition differences by precipitation type. *Environ. Sci. Technol.* **2017**, *51*, 2628–2634. [[CrossRef](#)]
22. Selin, N.E.; Jacob, D.J. Seasonal and spatial patterns of mercury wet deposition in the United States: Constraints on the contribution from North American anthropogenic sources. *Atmos. Environ.* **2008**, *42*, 5193–5204. [[CrossRef](#)]
23. Cossa, D.; Heimbürger, L.E.; Lannuzel, D.; Rintoul, S.R.; Butler, E.C.V.; Bowie, A.R.; Averty, B.; Watson, R.J.; Remenyi, T. Mercury in the Southern Ocean. *Geochim. Cosmochim. Acta* **2011**, *75*, 4037–4052. [[CrossRef](#)]
24. Agather, A.M.; Bowman, K.L.; Lamborg, C.H.; Hammerschmidt, C.R. Distribution of mercury species in the Western Arctic Ocean (U.S. GEOTRACES GN01). *Mar. Chem.* **2019**, *216*, 103686. [[CrossRef](#)]
25. Šolić, M.; Krstulović, N.; Šantić, D.; Šestanović, S.; Ordulj, M.; Bojanić, N.; Kušpilić, G. Structure of microbial communities in phosphorus-limited estuaries along the eastern Adriatic coast. *J. Mar. Biol. Assoc. United Kingd.* **2015**, *95*, 1565–1578. [[CrossRef](#)]
26. Živković, I.; Kotnik, J.; Šolić, M.; Horvat, M. The abundance, distribution and speciation of mercury in waters and sediments of the Adriatic Sea. *Acta Adriat.* **2017**, *58*, 165–186. [[CrossRef](#)]
27. Zvonarić, T. The cycling of Mercury through the marine environment of Kaštela Bay. In Proceedings of the FAO/UNEP/IAEA Consultation Meeting on the Accumulation and Transformation of Chemical Contaminants by Biotic and Abiotic Processes in the Marine Environment, La Spezia, Italy, 24–28 September 1990; Gabrielides, G.P., Ed.; UNEP/FAO/IAEA: Athens, Greece, 1991; pp. 369–381.
28. Kwokal, Ž.; Francišković-Bilinski, S.; Bilinski, H.; Branica, M. A comparison of anthropogenic mercury pollution in Kaštela Bay (Croatia) with pristine estuaries in Öre (Sweden) and Krka (Croatia). *Mar. Pollut. Bull.* **2002**, *44*, 1152–1157. [[CrossRef](#)]
29. Zore-Armanda, M. Some dynamic and hydrographic properties of the Kastela Bay. *Acta Adriat.* **1980**, *21*, 55–74.
30. Coale, K.H.; Heim, W.A.; Negrey, J.; Weiss-Penzias, P.; Fernandez, D.; Olson, A.; Chiswell, H.; Byington, A.; Bonnema, A.; Martenuk, S.; et al. The distribution and speciation of mercury in the California current: Implications for mercury transport via fog to land. *Deep Sea Res. Part. II Top. Stud. Oceanogr.* **2018**, *151*, 77–88. [[CrossRef](#)]
31. Penezić, A.; Milinković, A.; Bakija Alempijević, S.; Žužul, S.; Frka, S. Atmospheric deposition of biologically relevant trace metals in the eastern Adriatic coastal area. *Chemosphere* **2021**, *283*, 131178. [[CrossRef](#)]
32. Schlitzer, R. Ocean Data View. Available online: <https://odv.awi.de> (accessed on 15 July 2019).
33. Živković, I.; Fajon, V.; Kotnik, J.; Shlyapnikov, Y.; Obu Vazner, K.; Begu, E.; Šestanović, S.; Šantić, D.; Vrdoljak, A.; Jozić, S.; et al. Relations between mercury fractions and microbial community components in seawater under the presence and absence of probable phosphorus limitation conditions. *J. Environ. Sci.* **2019**, *75*, 145–162. [[CrossRef](#)]
34. US EPA. *Method 1631. Revision E: Mercury in Water by Oxidation, Purge and Trap, and Cold Vapor Atomic Fluorescence Spectrometry*; US EPA: Washington, DC, USA, 2002.
35. Bryant, K.; Akbar, M. An exploration of wind stress calculation techniques in hurricane storm surge modeling. *J. Mar. Sci. Eng.* **2016**, *4*, 58. [[CrossRef](#)]
36. Siudek, P.; Kurzyca, I.; Siepak, J. Atmospheric deposition of mercury in central Poland: Sources and seasonal trends. *Atmos. Res.* **2016**, *170*, 14–22. [[CrossRef](#)]
37. Yuan, S.; Chen, J.; Cai, H.; Yuan, W.; Wang, Z.; Huang, Q.; Liu, Y.; Wu, X. Sequential samples reveal significant variation of mercury isotope ratios during single rainfall events. *Sci. Total Environ.* **2018**, *624*, 133–144. [[CrossRef](#)] [[PubMed](#)]
38. Kotnik, J.; Horvat, M.; Ogrinc, N.; Fajon, V.; Žagar, D.; Cossa, D.; Sprovieri, F.; Pirrone, N. Mercury speciation in the Adriatic Sea. *Mar. Pollut. Bull.* **2015**, *96*, 136–148. [[CrossRef](#)] [[PubMed](#)]
39. Zhang, L.; Blanchard, P.; Gay, D.A.; Prestbo, E.M.; Risch, M.R.; Johnson, D.; Narayan, J.; Zsolway, R.; Holsen, T.M.; Miller, E.K.; et al. Estimation of speciated and total mercury dry deposition at monitoring locations in eastern and central North America. *Atmos. Chem. Phys.* **2012**, *12*, 4327–4340. [[CrossRef](#)]
40. Engle, M.A.; Tate, M.T.; Krabbenhoft, D.P.; Schauer, J.J.; Kolker, A.; Shanley, J.B.; Bothner, M.H. Comparison of atmospheric mercury speciation and deposition at nine sites across central and eastern North America. *J. Geophys. Res.* **2010**, *115*, D18306. [[CrossRef](#)]
41. Brown, R.J.C.; Pirrone, N.; van Hoek, C.; Horvat, M.; Kotnik, J.; Wangberg, I.; Corns, W.T.; Bieber, E.; Sprovieri, F. Standardisation of a European measurement method for the determination of mercury in deposition: Results of the field trial campaign and determination of a measurement uncertainty and working range. *Accredit. Qual. Assur.* **2010**, *15*, 359–366. [[CrossRef](#)]
42. Monperrus, M.; Tessier, E.; Amouroux, D.; Leynaert, A.; Huonnic, P.; Donard, O.F.X. Mercury methylation, demethylation and reduction rates in coastal and marine surface waters of the Mediterranean Sea. *Mar. Chem.* **2007**, *107*, 49–63. [[CrossRef](#)]
43. Dill, C.; Kuiken, T.; Zhang, H.; Ensor, M. Diurnal variation of dissolved gaseous mercury (DGM) levels in a southern reservoir lake (Tennessee, USA) in relation to solar radiation. *Sci. Total Environ.* **2006**, *357*, 176–193. [[CrossRef](#)]
44. Crocker, W.C.; Zhang, H. Seasonal and diurnal variation of air/water exchange of gaseous mercury in a Southern Reservoir Lake (Cane Creek Lake, Tennessee, USA). *Water* **2020**, *12*, 2102. [[CrossRef](#)]
45. Andersson, M.E.; Gårdfeldt, K.; Wängberg, I.; Sprovieri, F.; Pirrone, N.; Lindqvist, O. Seasonal and daily variation of mercury evasion at coastal and off shore sites from the Mediterranean Sea. *Mar. Chem.* **2007**, *104*, 214–226. [[CrossRef](#)]